Investigation of propagation of partial discharges in power transformers and techniques for locating the discharge

S.N. Hettiwatte, Z.D. Wang and P.A. Crossley

Abstract: The location of partial discharges in a power transformer can be determined based on the characteristics of the transfer function from the discharge source to the measuring terminal. Previous studies partially validated the technique using computer simulation and practical experiments based on a PD calibrator to represent a discharge signal. 'Real' discharges produced by insulation defect models were used to study how discharges propagate in an 11 kV plain-disc-type transformer winding. A corona model and a 'floating objects in oil' model produced discharge signals with different durations at various locations along the winding. Measurements were taken at the tap of the bushing capacitance through a conventional discharge detector. The signals were filtered, amplified and fed into a digital storage oscilloscope. The frequency spectra of the measured signals showed significant similarities irrespective of the type of discharge source. The characteristic of the transfer functions, i.e. the crests and troughs in the spectra, could be used for locating the source of the discharge. Energising the transformer increased the level of electric noise, which did affect the low frequency end of the spectra, but did not have any impact on the characteristics used for location.

1 Introduction

A significant percentage of the primary plant used in power networks in the developed world is now operating beyond its predicted design life. Ensuring that such equipment continues to operate safely and reliably is of crucial importance particularly when one considers the existing competitive/regulatory operating environment. Insulation faults are one of the main causes of equipment failure and are often preceded by partial discharges. A partial discharge (PD) is 'a localised electrical discharge that only partially bridges the insulation between conductors and which may or may not occur adjacent to a conductor' [1]. PD activity inside a power transformer can deteriorate the oil or paper insulation, degrade the voltage withstand capability and eventually lead to a catastrophic failure. Detecting and locating discharges at an early stage in their evolution can prevent an incipient insulation fault, facilitate maintenance and extend the safe operating life.

Partial discharge may occur in solid, liquid and gaseous insulation media and are generally initiated by an excessive localised electric field. The PD-induced current in an external circuit depends on the nature of the discharge and the geometry of the system [2]. Specifically, in a power transformer the most common sources of PD are gaseous discharges that occur in bubbles in oil or voids in paper/pressboard, surface discharges along oil/pressboard barriers or discharges caused by floating objects. The PD signals detected at the terminals of a transformer will have different waveshapes due to the different propagation paths from the discharge source to the terminals, even if the same type of discharge generates them.

Previous simulation studies [3] have suggested that the PD signals at the measurement terminals 'footprint' their propagation paths and the transfer functions from the source of the discharge to the measuring terminal have unique characteristics. The measurements conducted using PD calibrators on several plain-disc-type windings [4, 5] validated the simulation and confirmed that the characteristics of the transfer function can be extracted from the measurement signals and used for location purposes. A conventional discharge detector was used during those measurements.

Studies carried out on the transfer function based PD location techniques [5, 6] indicated the importance of developing these techniques into practical applications. In this paper experimental results obtained by energising an 11 kV transformer winding with various externally connected insulation defect models are presented. The resulting 'real' discharge signals help validate the transfer function based PD location technique and prove it is feasible to combine this location technique with measurements made by a conventional PD detector.

2 Characteristics of transfer functions

If a partial discharge occurs at position x_0 in the equivalent circuit of a winding as shown in Fig. 1, the currents at the bushing tap i_b and the earthed neutral i_g can be described

IEE Proceedings online no. 20050944
doi:10.1049/ip-smt:20050944
Paper first received 9th May 2003 and in revised form 14th May 2004

S.N. Hettiwatte and Z.D. Wang are with the School of Electrical Engineering and Electronics, University of Manchester, Manchester M60 1QD, UK
P.A. Crossley is with the School of Electrical and Electronic Engineering, Queen's University Belfast, Belfast BT9 5AH, UK
E-mail: zhongdong.wang@manchester.ac.uk

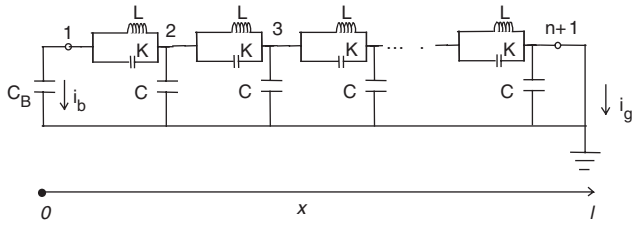

Fig. 1 *Equivalent circuit of single, uniform transformer winding*

by (1) and (2) [4]

$$i_b(j\omega) = \frac{\frac{C_B}{C} \cdot r \cdot \sinh(r(l - x_0))}{-\cosh(rl) + \frac{C_B}{C} \cdot r \cdot \sinh(rl)} \bullet i_{pd}(j\omega) \quad (1)$$

$$i_g(j\omega) = \frac{-\cosh(rx_0) + \frac{C_B}{C} \cdot r \cdot \sinh(rx_0)}{-\cosh(rl) + \frac{C_B}{C} \cdot r \cdot \sinh(rl)} \bullet i_{pd}(j\omega) \quad (2)$$

where

$$r^2 = \frac{-LC\omega^2}{1 - LK\omega^2} \quad (3)$$

C_B is the bushing capacitance, C, L, and K are the capacitance to earth, inductance and series capacitance of the winding per unit length and l is the total length of winding. These equations show that the transfer functions have fixed poles but different zeros, since the denominators are only related to the physical parameters of winding, i.e. C_B, C, l and r, while the numerators are also related to the location of the discharge source, i.e. x_0. Consequently the frequency positions of these zeros are related to the location of the discharge source and the positions of poles are determined by the overall winding construction and therefore are at fixed frequencies.

3 Transformer winding and defect models

The 11 kV transformer winding used in this study is a plain disc-type winding with 72 sections. Sections 1–32 and 41–72 had 7 + 11/12 turns per section and each turn consisted of double conductors of 6.0 × 2.0 mm. The remaining sections 33–40 had 6 + 1/2 turns per section and each turn consisted of double conductors of 5.0 × 2.6 mm. The thickness of insulation on all the conductors is 0.5 mm.

Two defect models were used in the experiments; one was a corona model and the other a 'floating objects in oil' model. They were connected at various locations on the winding and when energised used to study the discharge propagation characteristics. The corona model was used when the winding was energised directly to test the possible noise problem due to the operation of transformers.

Figure 2 shows the normalised 'real' discharge signals generated by the corona and floating objects models. The discharge waveform of the floating objects in oil has a rise and fall time of roughly 10 ns, while the corona has a similar rise time, approximately 6 ns, and a significantly slower fall time, roughly 150 ns for negative corona and 300 ns for positive corona.

Figure 3 shows the measured impedance of the circuit (11 kV winding + bushing capacitance) obtained using an impedance analyser. At high frequencies the transformer winding behaved as a *RLCG* network comprised of inductance L, capacitance C, and resistive R and dielectric G losses. Therefore the winding impedance increased or decreased, depending on whether the impedance was inductive or capacitive at that particular frequency. The

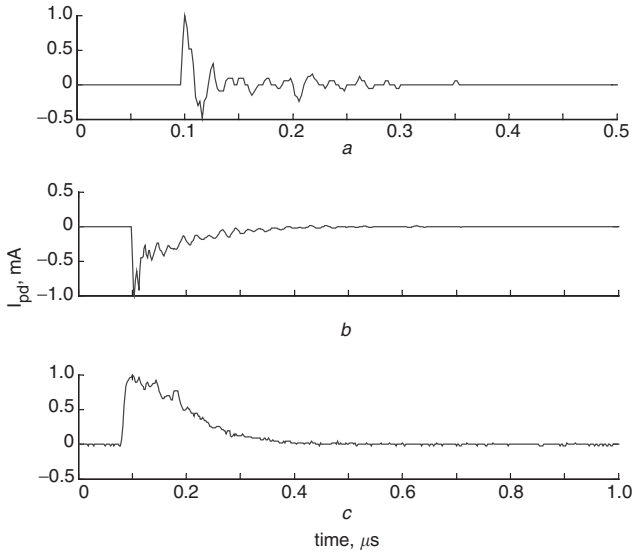

Fig. 2 *Normalised discharge waveforms*
a Floating objects in oil
b Negative corona
c Positive corona

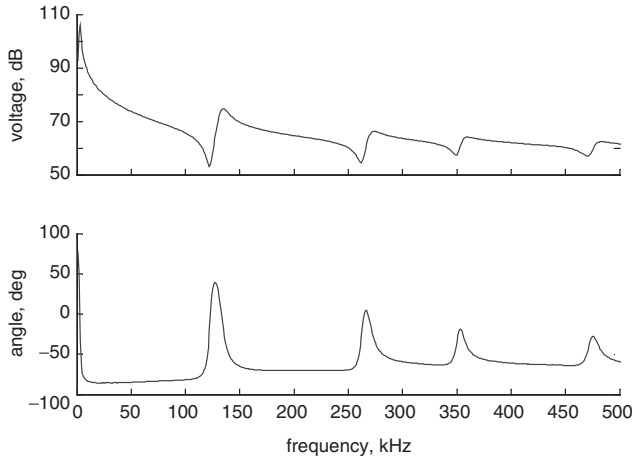

Fig. 3 *Measured impedance of circuit (11 kV winding + bushing capacitance)*

Table 1: Frequencies in kHz of crests of measured impedance in Fig. 3

r_1	r_2	r_3	r_4
126	269	356	476

frequencies of impedance crests vary according to the type of winding and its physical construction. Table 1 gives the frequencies of crests of measured impedance in Fig. 3.

4 Experiment results

4.1 Two types of discharges: corona and floating objects in oil

Figure 4 shows the test set-up used for investigating the propagation of 'real' discharges along the winding. The discharges were produced using insulation defect models energised at high voltages. The winding was connected in parallel with a discharge-free coupling capacitor $C_k = 333$ pF, chosen to simulate the bushing capacitance.

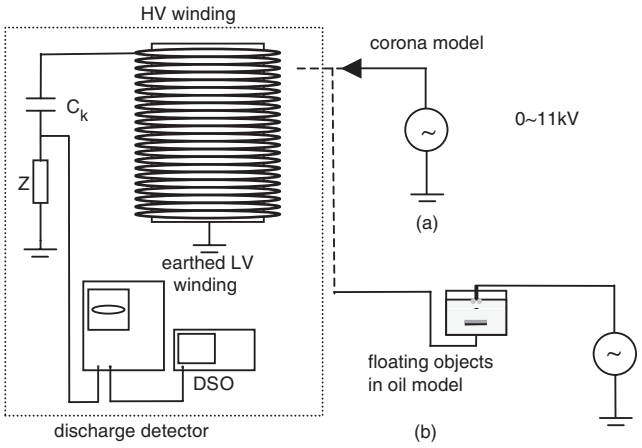

Fig. 4 *Experimental test set-up 1 and 2*
a Set-up 1
b Set-up 2

The measuring impedance Z was connected in series with C_k to measure the line-end signal of the winding. Signals picked up by Z were fed into the discharge detector which had a passband of $40 \sim 300$ kHz.

The filtered and amplified signals were not only observed on the ellipse of the detector, but were also brought out through a coaxial cable to a digital storage oscilloscope (DSO) used for recording the waveforms.

In Fig. 4*a* as the corona model was moved to different discs on the winding, the air gap between the point electrode and the outer insulated conductor was maintained at 10 mm. The effect of corona in the air gap was then measured at the tap of the bushing capacitance.

Figures 5*a* and 5*b* show the discharge signals measured at the line-end of the winding using the DSO. The location of the discharge is expressed in terms of the number of disc pairs from the line-end terminal. It can be seen from Fig. 5 that when the PD is located close to the line-end the shape of the measured signal is the response of the filter used within the detector. If the PD is located further away from the line-end the measured signal became more oscillatory due to the propagation path of the winding. The difference in the shape of the measured signal can be used to determine whether the discharge source is close to the line-end or deep down into the winding. A more precise location can be achieved by extracting the features that characterise the discharge location from the frequency spectrum of the measured signal.

The frequency spectra of the measured signals in Fig. 5 were computed using an FFT and 'corrected' using the inverse frequency characteristic of the band pass filter. These are shown in Fig. 6*a* and 6*b*. The crests of frequency spectra occurred at fixed frequencies, as given in Table 2. The troughs changed with the location of the PD source, for example the first trough for a PD at disc pair 4 was at 138 kHz and for disc pair 6 it moved to 142 kHz. The frequencies of the troughs increased as the location of the PD moved away from the measuring terminal at the line-end, as given in Table 3. It can be seen that the frequency of the first trough increased as the location of the PD moved up to disc pair 20, after which it disappeared. The region beyond disc pair 24, where the troughs are no longer observable was called the blind region. Within this region it is not possible to locate the precise position of PD. The blind area for the transfer function based location method can be explained by (4) and (5).

$$\begin{aligned} \sinh(r(l - x_0) &= 0 \\ \frac{LC\omega^2}{1 - LK\omega^2}(l - x_0)^2 &= k^2\pi^2 \end{aligned} \tag{4}$$

$$\begin{aligned} f_{zk} &= \frac{k}{2\sqrt{LC(l - x_0)^2 + LKk^2\pi^2}}, \quad k = 1, 2, ...n \\ f_{zk} &\approx \frac{1}{2\pi\sqrt{LK}} = f_c, \quad \text{when } x_0 \text{ approaches } l \end{aligned} \tag{5}$$

As the position of discharge x_0 approaches the neutral end of the winding (disc pair 36), i.e. l, the frequencies of the zeros of the transfer functions approach a single frequency as given in (5), which is called the critical frequency of the winding.

The test set-up shown in Fig. 4*b* corresponds to a floating objects in oil discharge. The winding was kept at earth potential and an oil vessel containing a point/pressboard/plate electrode with floating metal objects was energised at a high voltage. The floating objects, approximately 10 mm in diameter, were made using aluminium foil. The metal plate inside the oil vessel was connected to different taps along the winding. The line-end signals were then measured through the discharge detector. Although the discharge source of floating objects in oil is significantly different to the corona model, the measured signals were significantly similar to those shown in Fig. 5. For reasons of brevity, they are not included in the paper. Figure 7*a* and *b* show the frequency spectra of these signals.

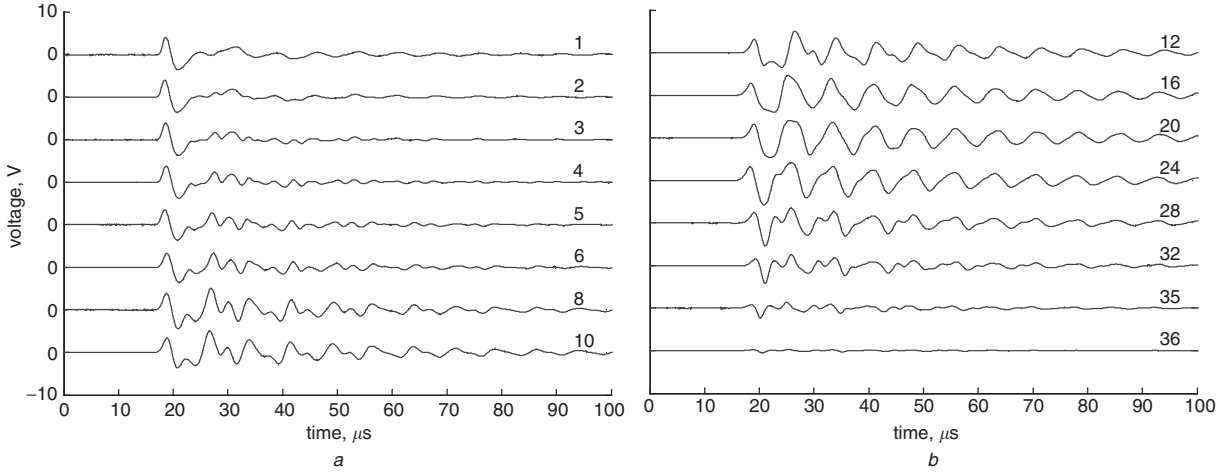

Fig. 5 *Line-end measured signals for test set-up 1*

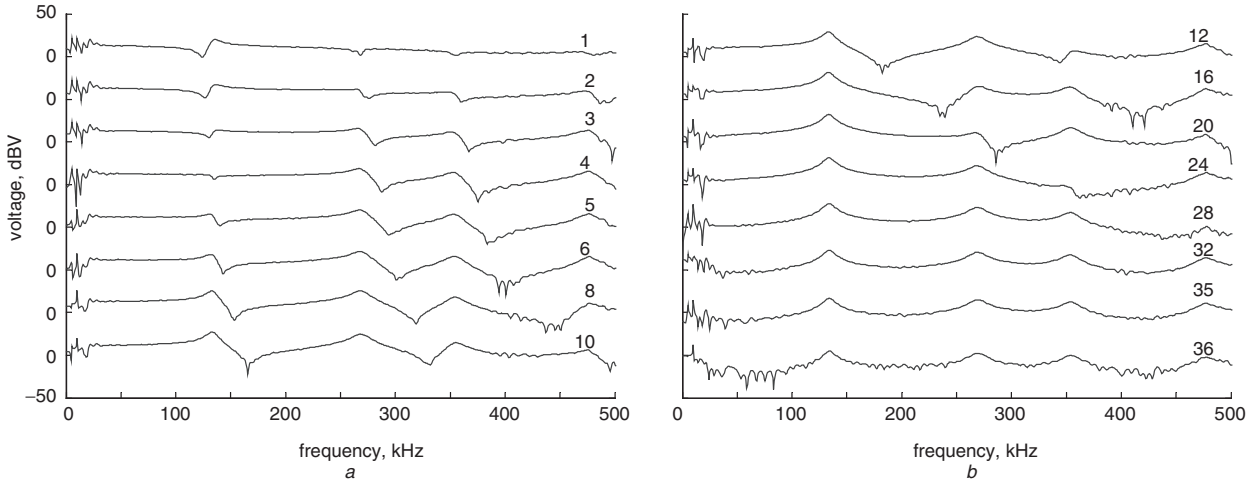

Fig. 6 *Frequency spectra of line-end signals for test set-up 1*

Table 2: Frequencies of crests in measured spectra shown in Fig. 6 (poles of transfer functions)

p_1	p_2	p_3	p_4
135	270	354	475

Table 3: Frequencies in kHz of troughs in measured spectra shown in Fig. 6 (zeros in transfer functions)

Disc pair	z_1	z_2	z_3
1	124	268	356
2	127	276	360
3	130	282	367
4	135	288	375
5	140	294	384
6	143	301	401
8	153	319	437
10	165	332	—
12	182	344	—
16	239	410	—
20	286	—	—

Although the original discharge signals obtained from corona and floating objects in oil had different durations and shapes, a conventional PD detector can only pick up their low-frequency components and cannot differentiate between them. This was regarded as the main deficiency in characterising a discharge source since durations and shapes of discharge signals were related to discharge mechanisms and were the main features for identification. An extra-wideband measurement system would be essential for discharge characterisation. However, it is an advantage in locating the discharge since the conventional discharge detector is only interested in the low frequency range of the discharge signals and within this range the 'footprint' of the propagation path would be dominant, irrespective of the type of discharge source. By comparing Fig. 7 with Fig. 6 it can be seen the spectra resulting from floating objects in oil is similar to corona. Frequencies of troughs in these frequency spectra are given in Table 4 and they are greatly similar to those given in Table 3.

4.2 Energising winding with defect models

The winding was energised using an 11 kV distribution transformer controlled by a variac. In Fig. 8*a*, a point electrode was directly connected to different taps along the winding with a 10 mm air gap to the earthed plate electrode. The model is designed to simulate discharges between a sharp conductive extrusion from the winding and the tank.

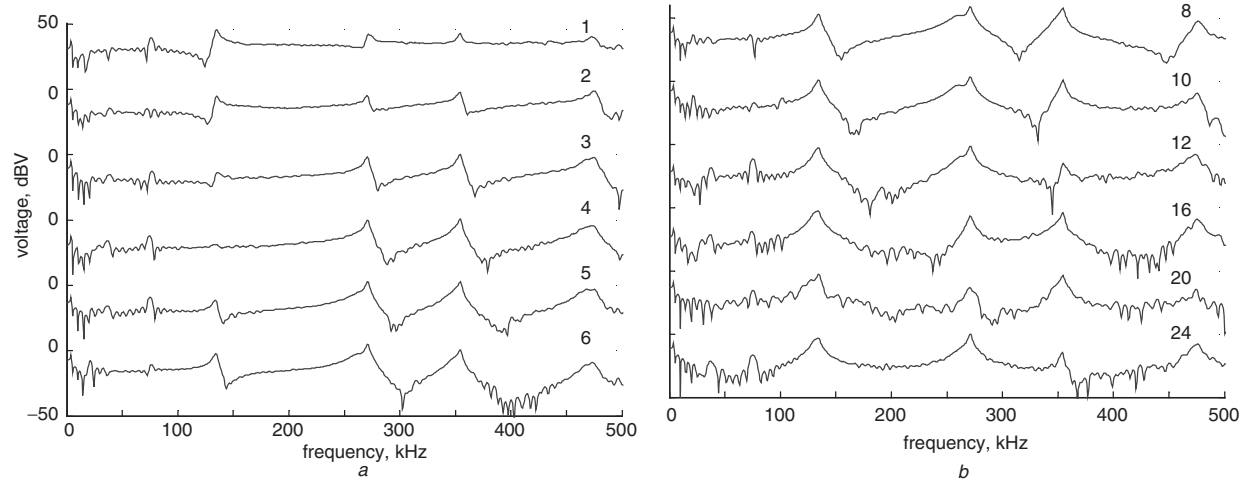

Fig. 7 *Frequency spectra of line-end signals for test set-up 2*

When the point–plane gap was connected to disc pair 1 corona incepted at a supplied voltage of 3.38 kV. In comparison when it was connected to disc pair 24, the corona incepted at 9.44 kV. Measurement of discharge activity could only be recorded for a point electrode connected to a disc pair between 1 and 24. Between 26 and 36 it was not possible to create a discharge using an 11 kV supply.

Table 4: Frequencies in kHz of troughs in measured spectra shown in Fig. 7 (zeros in transfer functions)

Disc pair	z_1	z_2	z_3
1	124	266	—
2	127	276	361
3	130	280	368
4	—	288	379
5	141	292	397
6	144	302	403
8	155	315	448
10	166	332	—
12	181	345	—
16	—	—	—
20	—	—	—

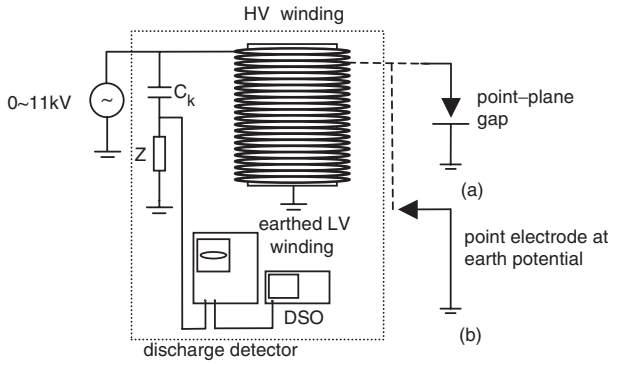

Fig. 8 *Experimental test set-up 3 and 4*
a Set-up 3
b Set-up 4

When the winding was energised there was significant audible and electrical noise due to core vibration, which was then detected by the monitoring circuit. The result was an increase in the noise level seen in the time domain signals. The corresponding frequency spectra in Fig. 9*a* and 9*b* show that the noise only affects the spectra in the lower frequency range, i.e. below 50 kHz. The features used for locating the discharge, i.e. the crests and troughs within the frequency band 100 to 500 kHz were not affected by the noise from the transformer. Table 5 also gives the frequencies of troughs in the spectra.

In Fig. 8*b* an earthed point electrode was used to simulate the effect of a sharp protrusion at earth potential. With this set-up, the discharge current generated near the point electrode had to couple through the main insulation and travel through the winding before reaching the line-end measuring terminal. Figure 10*a* and 10*b* show the frequency spectra, which has similar characteristics to those presented in Figs. 6, 7 and 9. Table 6 gives the frequencies of troughs in the spectra of Fig. 10 for comparision with Tables 3, 4 and 5. They show good agreement and indicate the zeros of transfer functions are the good features for location of discharge sources.

Table 5: Frequencies in kHz of troughs in measured spectra shown in Fig. 9 (zeros in transfer functions)

Disc pair	z_1	z_2	z_3
1	124	270	356
2	130	276	362
3	132	282	371
4	136	290	380
5	141	296	391
6	143	305	401
8	154	316	—
10	167	331	—
12	188	343	—
16	242	417	—
20	287	—	—

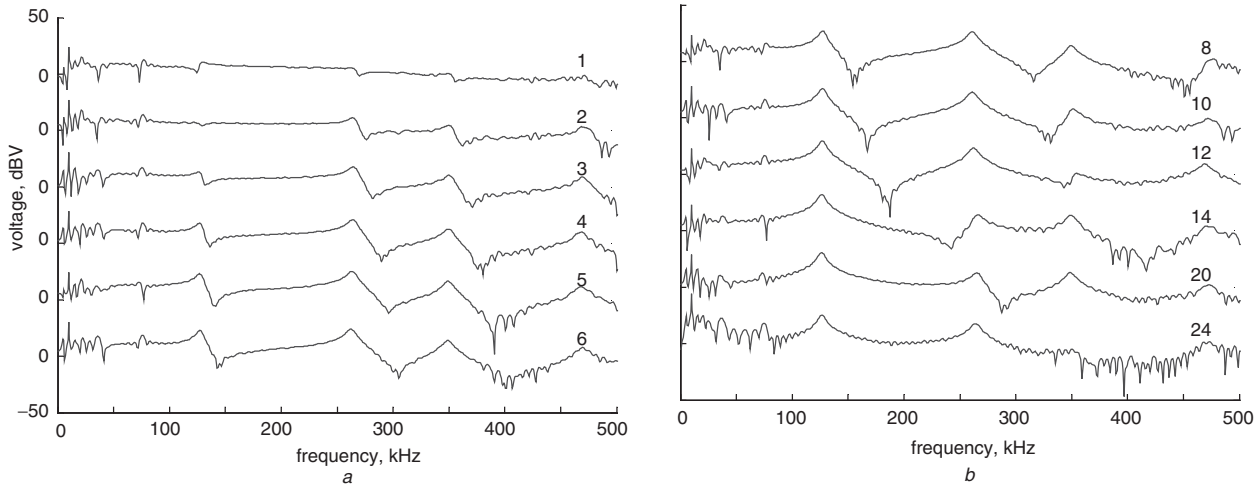

Fig. 9 *Frequency spectra of line-end signals for test set-up 3*

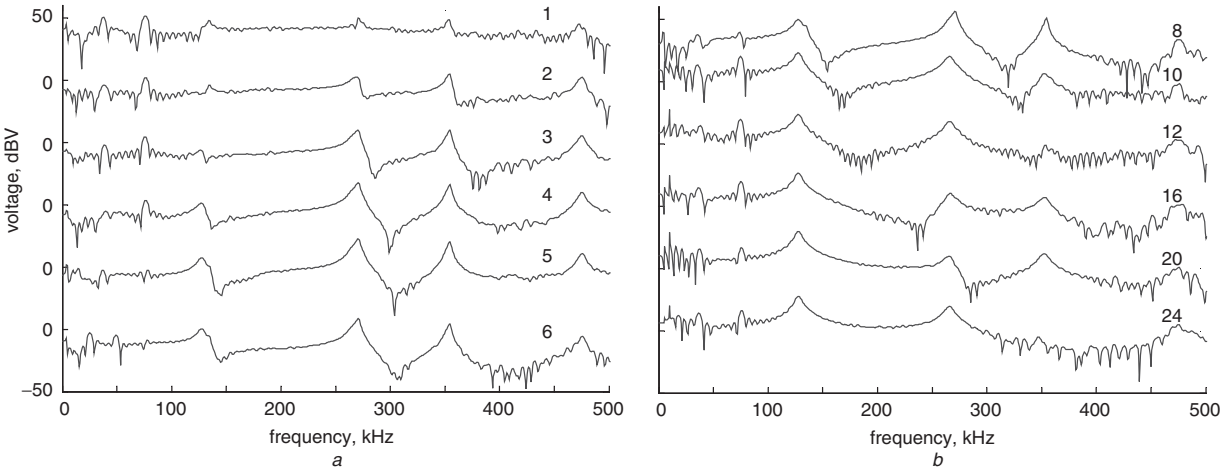

Fig. 10 *Frequency spectra of line-end signals for test set-up 4*

Table 6: Frequencies in kHz of troughs in measured spectra shown in Fig. 10 (zeros in transfer functions)

Disc pair	z_1	z_2	z_3
1	124	—	—
2	—	279	—
3	132	286	—
4	137	299	—
5	145	303	—
6	145	306	—
8	154	319	—
10	165	333	—
12	185	345	—
16	236	—	—
20	285	—	—

5 Conclusions

Real discharges produced when energising a corona model and floating objects in an oil model connected to an 11 kV plain disc-type transformer winding were used to study the propagation characteristics of partial discharges. Irrespective of the duration of the discharge signal generated by different types of discharges, the frequency spectra of the signals measured at the tap of bushing capacitance showed significant similiarites. The crests of the spectra always occurred at fixed frequencies, while the troughs changed in frequency with the position of the discharge source. As the discharge source was moved away from the measuring terminal, the frequencies of the troughs increase.

Although energising the transformer increased the level of electric noise, the noise only affected the low-frequency spectra, it did not affect the frequency characteristics used for location. Using a conventional discharge detector that extracts the low-frequency signals of the discharge, the transfer functions that describe the discharge propagation paths dominate the frequency range of the measured signals, irrespective of the type of discharge source. The proposed transfer function based location technique could be implemented using a conventional PD detector and a digital storage oscilloscope.

6 Acknowledgments

This work was financially and technically supported by National Grid, Alstom Transformers and Edison Mission First Hydro. The authors would especially like to thank Mr. P. Jarman, Mr. A. Darwin and Mr. G Edwards for their helpful comments and encouragement. The first author would like to thank the Open University, Sri Lanka in allowing him to study for a PhD degree at UMIST.

7 References

1 IEC60270: 'High-voltage test techniques - Partial discharge measurements' 3rd Edition, December 2000
2 Boggs, S.A.: 'Partial discharge: overview and signal generation', *IEEE Electr. Insul. Mag.*, 1990, **6**, (4), pp. 33–39
3 Wang, Z.D.: 'Location of partial discharges in power transformers'. PhD Thesis, UMIST, Manchester, UK, 1999
4 Wang, Z.D., Crossley, P.A., Cornick, K.J., and Zhu, D.H.: 'Partial discharge location in power transformers', *IEE Proc. Sci., Measur. Technol.*, 2000, **147**, (5), pp. 249–255
5 Hettiwatte, S.N., Wang, Z.D., Crossley, P.A., Darwin, A., and Edwards, G.: 'Experimental investigation into the propagation of partial discharge pulses in transformers', Presented at the IEEE Power Engineering Society Winter Meeting, New York, USA, January 2002
6 Debruyne, H., and Lesaint, O.: 'A method to locate a PD source in a winding by processing signals at its terminals'. Proc. 12th Int. Symp. on High Voltage Engineering (ISH'2001), Bangalore, India, August 2001
7 Akbari, A., Werle, P., Borsi, H., and Gockenbach, E.: 'Transfer function-based partial discharge localization in power transformers: a feasibility study', *IEEE Electr. Insul. Mag.*, 2002, **18**, (5), pp. 22–31